



1 **Impacts of anemometer changes, site relocations and**  
2 **processing methods on wind speed trends in China**

3 Yi Liu<sup>1</sup>, Lihong Zhou<sup>1</sup>, Yingzuo Qin<sup>1</sup>, Cesar Azorin-Molina<sup>2</sup>, Cheng Shen<sup>3</sup>, Rongrong

4 Xu<sup>1\*</sup>, Zhenzhong Zeng<sup>1\*</sup>

5 <sup>1</sup> School of Environmental Science and Engineering, Southern University of Science and Technology,  
6 Shenzhen, China

7 <sup>2</sup> Centro de Investigaciones sobre Desertificación, Consejo Superior de Investigaciones Científicas  
8 (CIDE, CSIC-UV-Generalitat Valenciana), Climate, Atmosphere and Ocean Laboratory (Climatoc-Lab),  
9 Moncada, Valencia, Spain

10 <sup>3</sup> Regional Climate Group, Department of Earth Sciences, University of Gothenburg, Gothenburg,  
11 Sweden

12

13 \* Correspondence: [xurr@sustech.edu.cn](mailto:xurr@sustech.edu.cn) (R. X); [zengzz@sustech.edu.cn](mailto:zengzz@sustech.edu.cn) (Z. Zeng)

14

Manuscript for *Atmospheric Measurement Techniques*

15

March 23, 2023

16



17 **Abstract**

18 *In-situ* surface wind observation is a critical meteorological data source for various  
19 research fields. However, data quality is affected by factors such as surface friction  
20 changes, station relocations, and anemometer updates. Previous methods to address  
21 discontinuities have been insufficient, and processing methods have not always adhered  
22 to World Meteorological Organization (WMO) guidelines. We analyzed data  
23 discontinuity caused by anemometer changes and station relocations in China's daily  
24 *in-situ* near-surface (~10m) wind speed observations and the impact of the processing  
25 methods on wind speed trends. By comparing the wind speed discontinuities with the  
26 recorded location changes, we identified 90 stations that showed abnormally increasing  
27 wind speeds due to relocation. After removing those stations, we followed a standard  
28 quality control method recommended by the World Meteorological Organization to  
29 improve the data reliability and applied Thiessen Polygons to calculate the area-  
30 weighted average wind speed. The result shows that China's recent reversal of wind  
31 speed was reduced by 41% after removing the problematic stations, with an increasing  
32 trend of  $0.017 \text{ m s}^{-1} \text{ year}^{-1}$  ( $R^2 = 0.64$ ,  $P < 0.05$ ), emphasizing the importance of robust  
33 quality control and homogenization protocols in wind trend assessments.

34 **Keywords.** wind speed trends; anemometer changes; station relocations; processing  
35 methods; quality control; homogenization

36



37 **1. Introduction**

38 *In-situ* surface wind observation is a key meteorological data that has been used in  
39 various avenues of research, e.g., wind power evaluation (Tian et al., 2019; Zeng et al.,  
40 2019; Liu et al. 2022a), extreme wind hazard monitoring and prevention (Zhou et al.,  
41 2002; Tamura, 2009; Liu et al., 2022b), and evapotranspiration analysis (Rayner, 2007;  
42 McVicar et al., 2012), to name but a few. The application of robust quality control and  
43 homogenization protocols are crucial for generating reliable wind speed time series for  
44 further trend and variability analyses (Azorin-Molina et al., 2014; Azorin-Molina et al.,  
45 2019).

46 Wind data quality is affected by surrounding surface friction change, station  
47 location issues, and anemometer changes in type and height (Masters et al., 2010; Wan  
48 et al., 2010; Cao & Yan, 2012; Hong et al., 2014; He et al., 2014; Azorin-Molina et al.,  
49 2018; Camuffo et al., 2020). Surrounding surface friction changes are mainly associated  
50 with urbanization (Zhang et al., 2022) and vegetation growth (Vautard et al., 2010),  
51 which modify wind speed fields around the stations. Because of these issues, stations  
52 are relocated to satisfy observing criteria (Trewin, 2010). Station relocation is quite  
53 common in rapidly developing countries. For instance, about 60% of stations in China  
54 experienced relocation (Sohu, 2004). Some relocation-caused breakpoints have been  
55 corrected by parallel observations (i.e. operating observations for an overlapping period  
56 at both the old and new observing stations; CMA, 2011; CMA, 2012; WMO, 2020), but  
57 not all (Feng et al., 2004; Fu et al., 2011; Patzert et al., 2016; Tian et al., 2019; Yang et  
58 al., 2021). Besides relocation caused by rapid urbanization (or vegetation growth),  
59 updates to automatic anemographs at the beginning of the 21<sup>st</sup> century in China also  
60 caused discontinuities in wind series (Fu et al., 2011).

61 Scientists have tried different methods to handle discontinuities. Tian et al. (2019)  
62 and Yang et al. (2021) deleted stations with recorded changes in latitudes, longitudes or  
63 altitudes, but they omitted to check whether those recorded relocations caused an abrupt  
64 discontinuity in the time series or if parallel observations have corrected them. This  
65 results in some stations being mistakenly deleted and significantly reduced the number



66 of available stations. Other research used statistical methods to detect or correct the  
67 time series' abnormal breakpoint (Feng et al., 2004; Wang, 2008). However, without  
68 examining the causes behind the discontinuity, this may also mistakenly delete stations  
69 with natural abrupt climatic changes (Bathiany et al., 2003). Combining those two  
70 methods by matching discontinuity with recorded station relocation is needed. Li et al.  
71 (2018) have manually checked the station histories for nine stations in North West  
72 China, but an algorithm is required to apply this approach to large datasets.

73 Besides data discontinuities, the processing method also affects the wind series.  
74 There are two critical steps in the processing: 1) selecting qualified stations and 2)  
75 calculating the average value. As for the first step, World Meteorological Organization  
76 (WMO) suggests deleting stations with either too much missing data or continuous  
77 missing data (WMO, 2017). Previous studies only constrained the number of missing  
78 values monthly (Zeng et al., 2019), yearly (Tian et al., 2019) or even in the whole period  
79 (Yang et al., 2021) but didn't check whether the missing values were continuous. As for  
80 the second step, most studies used the station average as the mean wind speed (Li et al.,  
81 2017; Zeng et al., 2019; Tian et al., 2019; Yang et al., 2021; Shen et al., 2021; Zha et  
82 al., 2021). However, station distribution and wind speed spatial variation are often  
83 inhomogeneous (Feng et al., 2004; Fu et al., 2011; Liu et al., 2019). Therefore the  
84 station average will have spatial biases. An improved average method to rearrange the  
85 weight for each station, e.g. Thiessen Polygon (Fu et al., 2011), is needed.

86 Herein, taking stations in China as an example, we analyzed the existing data  
87 discontinuities and their potential causes. Furthermore, we propose an improved  
88 solution by using an algorithm to compare the statistic breakpoint with the recorded  
89 relocation to double-check the discontinuity caused by relocation. Then using WMO's  
90 quality control criteria and Thiessen Polygon (Thiessen, 1911), we generated wind  
91 speed time series without temporal bias caused by heterogeneous missing values and  
92 spatial biases caused by uneven station distribution.

93

## 94 **2. Dataset and methodology**



95 **2.1 WMO quality control method**

96 We used the China Surface Climatic Data Daily Data Set (CSD) (Version 3.0) from  
97 the China Meteorological Data Service Center (<http://data.cma.cn/en/?r=data/>; last  
98 accessed March 2020). The quality control method is recommended by WMO (2017),  
99 which required the following criteria before using the daily mean values in a month as  
100 monthly mean values: (1) <11 missing daily values in a month and (2) <5 consecutive  
101 missing daily values in a month. Qualifying stations must have monthly values for  
102 every month during the study period; Otherwise, the station will be completely  
103 excluded from the calculation. The station excluded by each criterion can be found in  
104 Table S1.

105

106 **2.2 Station location changes in record**

107 CSD provides daily wind speed and location information for 840 stations for 1961-  
108 2019. But there are some mistakes in the daily location records. For example, if the  
109 station location changed from A to B and back to A within a month, B is potentially a  
110 mistaken record. Therefore, we first use mode (the statistic term meaning the value that  
111 appears most often, here referring to the location with the highest frequency in a month)  
112 to resample the daily location to the monthly location. Second, considering that  
113 recorded longitude and latitude has the same spatial resolution of minutes, we defined  
114 the threshold of location change as the minimum accuracy of the longitude and latitude  
115 record, i.e., one minute. That is 1.85km for longitude and  $1.85\text{km} \cdot \cos\varphi$  for latitude,  
116 where  $\varphi$  is the latitude. Third, as for altitude, we allow a 20m measuring error following  
117 Tian et al. (2019). A station with more than 20m change in altitude will be considered  
118 as relocation. It is noteworthy that CSD labels uncertain altitude records by adding  
119 10km to the raw data (CMA, 2017), which are considered as no observations in our  
120 analysis. This way, we identified 432 stations as relocations from the 601 qualified  
121 stations after applying the WMO quality control (details in Table S2).

122

123 **2.3 Breakpoint detection and the comparison with recorded relocation**



124 We used Pruned Exact Linear Time (PELT) method (Killick, Fearnhead & Eckley,  
125 2012) to detect the jumps in the mean level in the monthly wind speed time series (Fig  
126 4a, Fig 4c). This method is a wrapped function named *findchangepts* in Matlab. PELT  
127 is essentially a traversing method. For a time series with N values ( $x_1, x_2 \dots x_N$ ), the  
128 function uses equations 1 & 2 to calculate the total residual errors ( $J$ ) for each point ( $k$ )  
129 assumed as a breakpoint. The point with the most significant change in the mean (lowest  
130 total residual errors,  $J$ ) is reported as the breakpoint. The breakpoints here can be caused  
131 by artificial relocations or natural climate changes.

$$132 \quad J(k) = \sum_{i=1}^{k-1} (x_i - \text{mean}([x_1 \dots x_{k-1}]))^2 + \sum_{i=k}^N (x_i - \text{mean}([x_k \dots x_N]))^2 \quad (1)$$

$$133 \quad \text{mean}([x_m \dots x_n]) = \frac{1}{n-m+1} \sum_{r=m}^n x_r \quad (2)$$

134 Then we use relocation records to separate changes brought by artificial relocation  
135 from changes in natural climate. If the breakpoint and one of the relocation dates (some  
136 stations have more than one relocation record) happened in the same two months, we  
137 will consider that the time series is significantly affected by the relocation, and the  
138 station will be deleted. Stations with natural-climate-caused location changes will be  
139 reserved.

140 The change point in the trend of the annual national average wind speed (Fig 2b,  
141 Fig 5b) is detected following the method used by Wang et al. (2011). All the trends  
142 reported are based on the least square fits.

143

### 144 **3. Results and discussion**

#### 145 **3.1 Data issue due to anemometer changes**

146 We found a clear decline in the frequency of zeros in most CSD stations between  
147 2002 and 2007 (Figure 1a), from 10-14 days per year to less than two days per year.  
148 This clear drop is not a result of wrongly taking zero values as no observations (NaN)  
149 as happened in the Integrated Surface Dataset (ISD, Dunn et al., 2022), as no abrupt  
150 increase in NaN frequency was observed (Supplementary Figure S1). Instead, the  
151 decline is accompanied by an improvement in record accuracy: i.e., the measurement

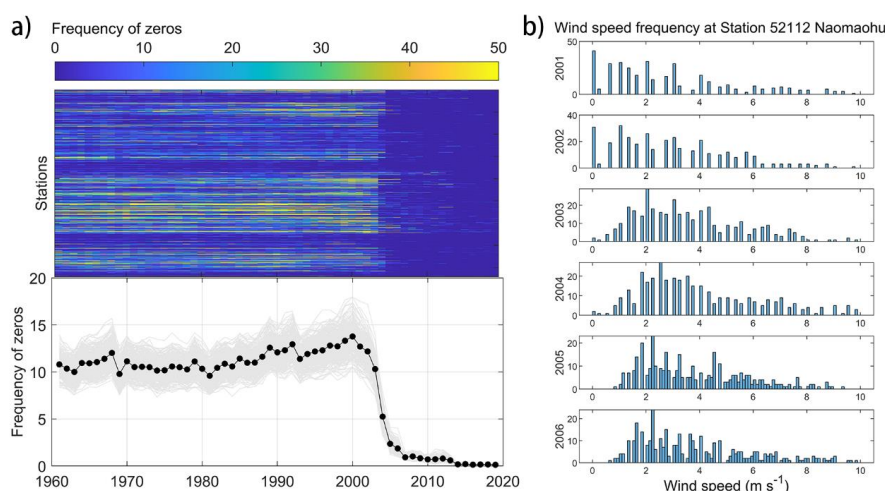


152 intervals became narrow (from 0, 0.3, 0.5, 0.7, 0.8, 1.0 m s<sup>-1</sup>, etc. to 0, 0.1, 0.2, 0.3 m  
153 s<sup>-1</sup>, etc.; Figure 1b and Supplementary Figure S2). Taking Station Naomaohu in  
154 Xinjiang (station ID: 57432) as an example, from 2002 to 2003, zero values decreased  
155 from more than 30 days per year to less than five days per year and wind speed records  
156 changed from 0, 0.3, 0.7, 1.0 m s<sup>-1</sup>, etc. to 0, 0.3, 0.5, 0.8, 1.0 m s<sup>-1</sup>, etc. Since 2004, the  
157 record accuracy was further improved to 0.1, 0.2, 0.3... m s<sup>-1</sup> and zeros values almost  
158 disappeared (Figure 1b).

159 This change is potentially caused by the transformation in measure frequency,  
160 anemometer type and data logging, based on the station history recorded by Xin et al.  
161 (2012). As for measurement frequency, in 2003, Station Naomaohu changed from 3  
162 observations per day (i.e., 8:00, 14:00 and 20:00, China Standard Time) to four times  
163 per day (2:00, 8:00, 14:00 and 20:00, China Standard Time). The increase in the  
164 frequency of measurements decreases zeros in daily wind data, as only if all  
165 observations report zero wind speeds, will the daily data (i.e., the average of all  
166 observations in a day; CMA, 2017) be recorded as zero. Then in 2005, the EL contact  
167 anemograph (Yang, 1986; Jin, 2011; Xin et al., 2012, Zhang et al., 2020) requiring  
168 manual recording was changed to EC photoelectric encoder self-recording type (Kuang,  
169 2016; Jin, 2011; Xin et al., 2012). Both EL and EC type anemographs use cup  
170 anemometers to measure wind speed. This anemograph change further decreases the  
171 likelihood of recording zero daily wind speed because the updated new anemometers  
172 are more sensitive, and even very low wind speeds will be measured with a value  
173 instead of recorded as zero (Azorin-Molina et al., 2018). The smooth increasing  
174 frequency of zero values from 1960 until 2000 also supports this statement (Figure 1a):  
175 the longer the anemometer is used, the less sensitive it will become, and hence a greater  
176 wind speed will be required to record a non-zero value (Azorin-Molina et al., 2018),  
177 overall increasing the zero values. As for the change in data accuracy, there are two  
178 reasons: 1) EL type anemograph only measures the times of electronic contact (200  
179 meters rotation distance per contact) in 10 mins, therefore it has discrete records. For  
180 example, one contact means 0.3 m s<sup>-1</sup> (200m/600s) and two contacts means 0.7 m s<sup>-1</sup>



181 (400m/600s) (Hu et al., 2009) while EC type has more accurate records using the Grey  
182 Code; 2) the data logging changed from manual reading, calculating and rounding to  
183 instrument automatically calculating and retaining one decimal place.



184  
185 **Figure 1. Changes in wind speed data caused by anemometer updates. a)** Decrease of  
186 frequency of zeros. Each horizontal bar in the upper figure represents one station and  
187 there are 840 stations in total. The color indicates the frequency of zeros (days per year).  
188 The black dotted line in the lower figure is the average annual frequency of zeros of all  
189 the stations. The 300 grey lines are sample averages, each containing 40% amount of  
190 the total stations. **b)** Frequency (days per year) of daily wind speed measurements  
191 between 2001 and 2006 for Station #52112 Naomaohu (43°45'N, 94°59'E, 479.0 m  
192 a.s.l.)

193  
194 **3.2 Quality-controlled series**

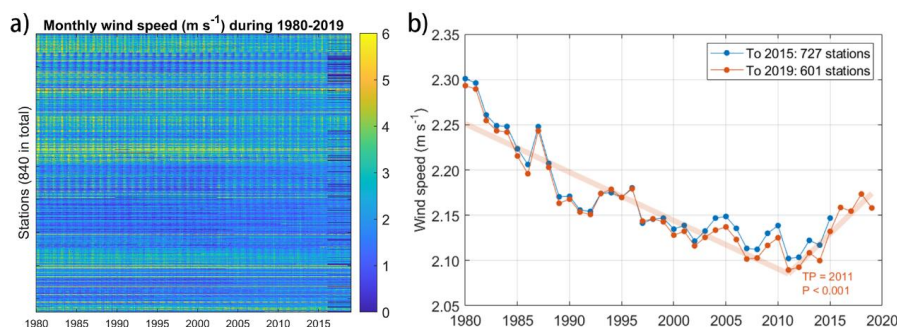
195 Following WMO's criteria, we generated the monthly average wind speed for each  
196 station (Figure 2a). We found that since January 2016, there have been 126 stations that  
197 no longer have records (distribution see Figure S3). We compared the time series with  
198 and without these stations and found the difference is not significant (t-test  $P < 0.001$ ,  
199 Figure 2b). To obtain a longer time series including recent years' data, we deleted the  
200 126 stations and only used the 601 stations with complete monthly average wind speeds





201 for 1980-2019. The breakpoint was detected in 2011 ( $P < 0.001$ ) with a decreasing trend  
202 of  $-0.011 \text{ m s}^{-1} \text{ year}^{-1}$  ( $R^2 = 0.84$ ,  $P < 0.001$ ) before the breakpoint and an increasing  
203 trend of  $+0.022 \text{ m s}^{-1} \text{ year}^{-1}$  ( $R^2 = 0.87$ ,  $P < 0.001$ ) after.

204



205

206 **Figure 2. Monthly average wind speed after being filtered by WMO's criteria. a)**  
207 Each horizontal bar represents one station. Months with no data (NaNs) are represented  
208 by the deepest blue. **b)** Comparison of the monthly average wind speed for the short-  
209 (1980-2015; 727 stations) and long-period (1980-2019; 601 stations)

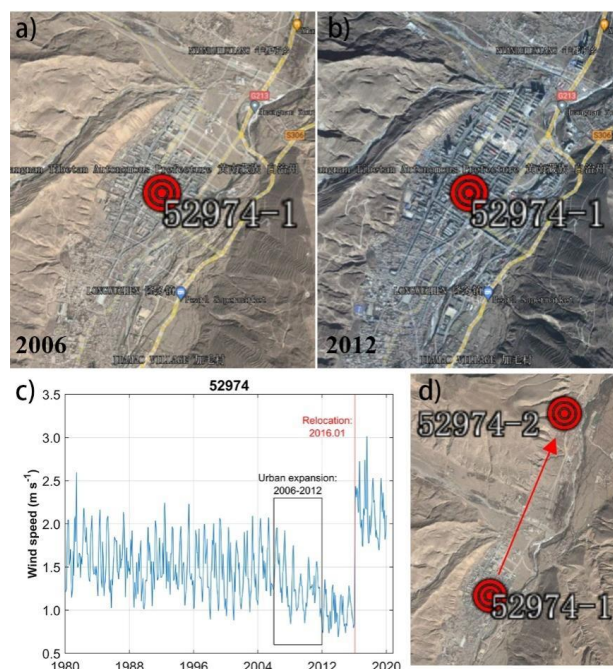
210

### 211 3.3 Station relocations caused by urbanization

212 Another key factor influencing wind speed measurements is the relocation of  
213 stations. We found that there is a clear data jump caused by relocations in some of the  
214 stations. Taking the station located in Qinghai (station ID 52974) as an example, we  
215 detected an abrupt jump in wind speed in January 2016. This date coincides with the  
216 relocation of the station from  $35^{\circ}31'N$ ,  $102^{\circ}01'E$  (ID 52974-1) in December 2015 to  
217  $35^{\circ}33'N$ ,  $102^{\circ}02'E$  (ID 52974-2) in January 2016 (Figures 3c & 3d). The relocation is  
218 potentially attributed to the urban growth around the station. As viewed by satellite  
219 images from Google Earth Pro, there is a rapid urban expansion from 2006 (Figure 3a)  
220 to 2012 (Figure 3b), especially towards the Northeast of the station, during wind speed  
221 records also experienced a decrease (Figure 3c). A similar decrease in both daily mean  
222 wind speed and maximum wind speed caused by urbanization was also reported in the  
223 Yangtze River region (Zhang et al., 2022). To eliminate the effect of buildings on the  
224 wind speed measurements, Station 52974 was moved to 4 km away from its previous



225 location (Figure 3d) so that wind speed is properly measured without artificial obstacles  
226 in the surroundings.  
227



228  
229 **Figure 3. Example of station relocation caused by rapid urbanization growth. a-b)**  
230 Landsat images crop from © Google Earth near Station 52974 in 2006 and 2012,  
231 respectively. **c)** the wind speed change with urbanization and relocation. **d)** Landsat  
232 images of the station relocation crop from © Google Earth.

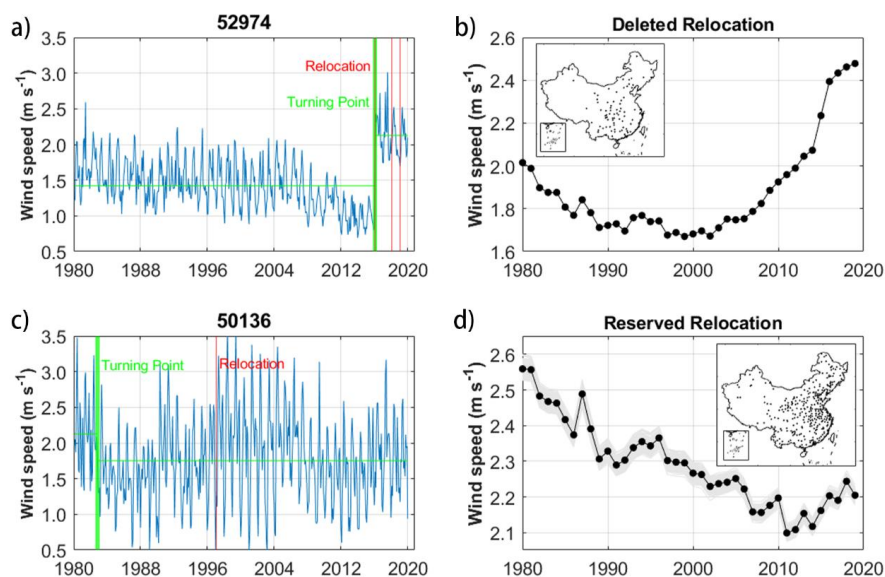
233  
234 Though some stations were influenced by station relocation as shown in Figure 3,  
235 a larger fraction (79%) of stations show no change in wind speed after the relocation.  
236 Further checking the raw record of locations for those stations, we find that one reason  
237 is that some “relocations” result from wrong location records. For example, Station  
238 52974 is mistakenly detected with three relocations (Figure 4a). However, only the first  
239 relocation is real and the latter two are results of location encoding change from 10202  
240 (interpreted as 102°02′) to 1022 (interpreted as 10°22′) and back. Another possible  
241 reason is that the relocation did happen but the data has been corrected. According to



242 the *Provisional Regulations on Relocation, Construction and Removal of National*  
243 *Ground Meteorological Observation* announced by China’s government in 2012,  
244 station relocations should have 1-2 years of parallel observations for data correction  
245 (CMA, 2012). This process may fix some of those discontinuities but not all (Feng et  
246 al., 2004; Fu et al., 2011; Patzert et al., 2016; Tian et al., 2019; Yang et al., 2021). For  
247 example, Station 59287, the only national basic weather station in Guangzhou,  
248 experienced two relocations in both 1996 and 2011, which is confirmed by the metadata  
249 (CMA, 2011). After correction, the 1996 relocation doesn’t show a sharp breaking point  
250 but the 2011 one does (Supplementary Figure S4).

251 To examine whether the relocation caused a substantial change in the wind speed  
252 record, we identified the most abrupt change in the wind speed time series and checked  
253 whether a relocation happened near the change point (see details in *Methods 2.3*). Out  
254 of the 432 relocated stations, 90 were deleted because the most significant shift in mean  
255 is at the time of the relocation, and hence this is the most likely cause. We then took the  
256 average of the “deleted relocation” stations and “reserved relocation” stations  
257 separately. The “deleted relocation” group shows an abnormally rapid increase in the  
258 recent two decades (Figure 4b). While the “reserved relocation” group is similar to  
259 stations without relocation (Supplementary Figure S5). To exclude the impact of  
260 different station counts in each category (fewer stations mean higher sensitivity to the  
261 individual abnormal station), we performed 300 samples using a random draw of 90  
262 stations from the “reserved relocation” group and showed them in grey lines in Figure  
263 4d. None of the grey lines shows an abnormal trend as the “deleted relocation” group.  
264 This proves that our method is efficient in identifying problematic stations.

265



266

267 **Figure 4. Comparison of deleted relocated stations and reserved ones.** a) The wind  
268 speed data breakpoint and relocations of one example of deleted relocation, Station  
269 52974. b) The station average wind speed of 90 deleted relocated stations. The inset  
270 shows the station distribution across China. c) One example of reserved relocation,  
271 Station 50136. d) The station average wind speed of 342 reserved relocated stations.  
272 The grey lines are the averages of 300 samples, each with 90 randomly drawn reserved  
273 relocated stations. Maps information are from Department of Natural Resources  
274 standard map service system of China.

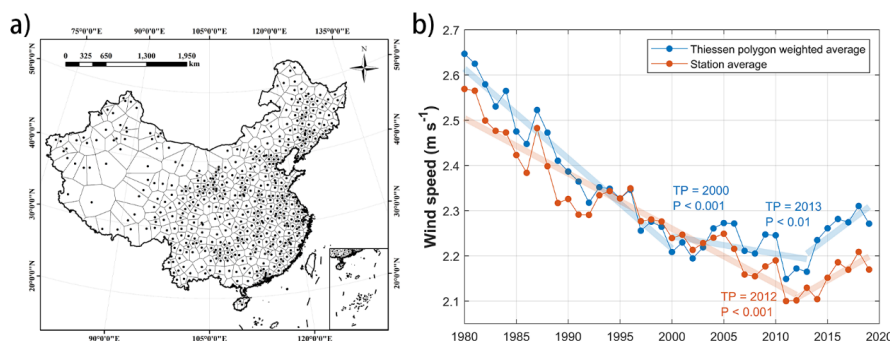
275

### 276 3.4 Average method used to calculate the national average

277 In the station average time series, the breakpoint was detected in 2012 ( $P < 0.001$ )  
278 with a trend of  $-0.012 \text{ m s}^{-1} \text{ year}^{-1}$  ( $R^2 = 0.90$ ,  $P < 0.001$ ) before and  $+0.013 \text{ m s}^{-1} \text{ year}^{-1}$   
279 ( $R^2 = 0.70$ ,  $P < 0.01$ ) after (Figure 5b). The increasing trend decreased by 41% after  
280 deleting those relocation-affected stations, compared with the  $+0.022 \text{ m s}^{-1} \text{ year}^{-1}$  in  
281 Figure 2b (also reported by Liu et al., 2022a). But the trend is larger than the  $+0.011 \text{ m}$   
282  $\text{s}^{-1} \text{ yr}^{-1}$ , reported by Yang et al. (2021), with all the recorded location changed stations  
283 deleted without checking whether the station is affected by the relocation.



284 We further used Thiessen Polygon (Thiessen, 1911) to give different weights to  
285 each station according to their representing area, i.e., large weight for stations located  
286 in sparse stations area (Figure 5a) and compare the result with the station average  
287 (Figure 5b). Thiessen Polygon is essentially the finest divided subregion, which splits  
288 the region into the smallest representative area and ensure there is a station in each  
289 subregion. The Thiessen polygon weighted average is overall higher than the station  
290 average. This can be explained by the increasing weight of stations in North West China  
291 with higher wind speeds (Liu et al., 2019). While in the Thiessen polygon weighted  
292 average time series, there are two breakpoints in 2000 ( $P < 0.001$ ) and 2013 ( $P < 0.01$ ).  
293 The trend changes from quick decrease ( $-0.020 \text{ m s}^{-1} \text{ year}^{-1}$ ,  $R^2 = 0.94$ ,  $P < 0.001$ ) to  
294 unstable moderate decrease ( $-0.004 \text{ m s}^{-1} \text{ year}^{-1}$ ,  $R^2 = 0.17$ ,  $P = 0.14$ ) and quickly  
295 increase ( $+0.017 \text{ m s}^{-1} \text{ year}^{-1}$ ,  $R^2 = 0.64$ ,  $P < 0.05$ ). The increasing trend in the recent  
296 decade increased by 31% (from  $+0.013 \text{ m s}^{-1} \text{ year}^{-1}$  to  $+0.017 \text{ m s}^{-1} \text{ year}^{-1}$ ) after using  
297 the Thiessen polygon approach.



298  
299 **Figure 5. Thiessen polygons and the comparison between Thiessen polygon**  
300 **weighted average and station average.** a) The Thiessen polygon map of the 511  
301 qualified stations. b) The comparison of station average wind speed (orange line) and  
302 Thiessen polygon weighted average (blue line) across China for 1980-2019. The linear  
303 fitting models are shown in translucent thick lines accordingly. Maps information are  
304 from Department of Natural Resources standard map service system of China.

305

#### 306 4. Conclusions



307 Continuity is crucial for meteorological observation data. However, either the  
308 updates in the anemograph, the relocation caused by urbanization or the methods of  
309 data logging will affect wind speed data continuity. In this study, we comprehensively  
310 examined the discontinuity in wind speed data using a Chinese dataset. We found that  
311 updates to the automatic anemometer improved the observation frequency and  
312 instrument sensitivity, decreasing the zero-value daily wind speed data and increasing  
313 data accuracy. We also propose comparing the discontinuity in time series with recorded  
314 station relocation to check whether a relocation caused a breakpoint. We found that 90  
315 stations were affected by the relocation and show a quickly increasing wind speed in  
316 the recent two decades. After excluding those problematic stations, the wind speed  
317 reversal trend is reduced by 41% but still strong ( $P < 0.001$ , with an increasing trend of  
318  $+0.013 \text{ m s}^{-1} \text{ year}^{-1}$ ). The increasing trend reaches  $+0.017 \text{ m s}^{-1} \text{ year}^{-1}$  ( $R^2 = 0.64$ ,  $P <$   
319  $0.05$ ) after using Thiessen Polygon, which gives the stations in North West China a  
320 larger weight because their small number but located in a large area,

321 Though lots of methods (Masters et al., 2010; Wan et al., 2010; Cao & Yan, 2012;  
322 Hong et al., 2014; He et al., 2014; Azorin-Molina et al., 2018; Camuffo et al., 2020)  
323 were proposed to handle those problems, a comprehensive summary of them is lacked.  
324 This study fills this research niche. However, it is hard for external researchers to  
325 provide a better solution without a collaboration with National Weather Services and  
326 the access to station data records and/or metadata. Therefore, we hope National Weather  
327 Services could improve the data quality based on these feedbacks and complete the  
328 process by introducing an R package with open-source code on GitHub. This way, not  
329 only the data is easier to get and process, but also researchers can contribute to improve  
330 the dataset. One such example is the “rnpn” package to access and process USA  
331 National Phenology Network data (<https://github.com/usa-npn/rnpn>). Anyway, all raw  
332 data processing has limitations and adds additional uncertainty. As we keep reporting  
333 problems in datasets and improving our processing method, we should also pay more  
334 attention to increasing the quality and homogeneity of the wind data. This requires  
335 raising awareness of the importance of protecting the environment around the



336 observation station and avoiding relocations.

337



338 **Supplemental Information**

339 Document S1. Supplemental Information, Table S1, Figures S1 – S5.

340

341 **Acknowledgements**

342 Thanking Robert Dunn (UK Met Office) for discussions and comments on the  
343 manuscript. The authors wish to acknowledge the reviewers for their detailed and  
344 helpful comments to the original manuscript.

345

346 This study was supported by the National Natural Science Foundation of China (grant  
347 no. 42071022), the Swedish Formas (2019–00509 and 2017–01408) and VR (2021–  
348 02163 and 2019–03954), and the start-up fund provided by Southern University of  
349 Science and Technology (no. 29/Y01296122). C. A-M. was supported by VENTS  
350 (GVA-AICO/2021/023), the CSIC Interdisciplinary Thematic Platform (PTI) Clima  
351 (PTI-CLIMA), the 2021 Leonardo Grant for Researchers and Cultural Creators, BBVA  
352 Foundation, and the “Unidad Asociada CSIC-Universidad de Vigo: Grupo de Física de  
353 la Atmosfera y del Océano”.

354

355 **Data availability statement**

356 The data that support the findings of this study are available upon request from the  
357 authors.

358

359 **Author contributions**

360 **Zhenzhong Zeng:** Conceptualization, Methodology **Yi Liu:** Methodology, Software,  
361 Writing – Draft **Lihong Zhou:** Methodology, Data Curation **All other authors:** Writing  
362 – Review & Editing

363

364 **Declaration of interest**

365 The authors declare no competing financial interests.

366





367 **References.**

- 368 1. Azorin-Molina, C., Asin, J., McVicar, T. R., Minola, L., Lopez-Moreno, J. I.,  
369 Vicente-Serrano, S. M., & Chen, D. (2018). Evaluating anemometer drift: A  
370 statistical approach to correct biases in wind speed measurement. *Atmospheric*  
371 *research*, **203**, 175-188.
- 372 2. Azorin-Molina, C., Guijarro, J. A., McVicar, T. R., Trewin, B. C., Frost, A. J., &  
373 Chen, D. (2019). An approach to homogenize daily peak wind gusts: An application  
374 to the Australian series. *International Journal of Climatology*, **39**(4), 2260-2277.
- 375 3. Azorin-Molina, C., Vicente-Serrano, S. M., McVicar, T. R., Jerez, S., Sanchez-  
376 Lorenzo, A., López-Moreno, J., ... & Espírito-Santo, F. (2014). Homogenization  
377 and Assessment of Observed Near-Surface Wind Speed Trends over Spain and  
378 Portugal, 1961–2011, *Journal of Climate*, **27**(10), 3692-3712.
- 379 4. Bathiany, S., Scheffer, M., Van Nes, E. H., Williamson, M. S., & Lenton, T. M.  
380 (2018). Abrupt climate change in an oscillating world. *Scientific reports*, **8**(1), 1-  
381 12.
- 382 5. Camuffo, D., della Valle, A., Becherini, F., & Zanini, V. (2020). Three centuries of  
383 daily precipitation in Padua, Italy, 1713–2018: history, relocations, gaps,  
384 homogeneity and raw data. *Climatic Change*, **162**(2), 923-942.
- 385 6. Cao, L. & Yan, Z. (2012). Progress in research on homogenization of climate data.  
386 *Advances in Climate Change Research*, **3**(2), 59-67.
- 387 7. China Meteorological Administration (CMA, 2017). *Meteorological data set*  
388 *description document*. [In Chinese]
- 389 8. China Meteorology Administration (CMA, 2011). National Basic Meteorological  
390 Station in Guangzhou was relocated four times in 62 years, *Media attention*,  
391 Retrieved from:  
392 [http://www.cma.gov.cn/2011xwzx/2011xmtjj/201110/t20111026\\_121807.html](http://www.cma.gov.cn/2011xwzx/2011xmtjj/201110/t20111026_121807.html).  
393 [In Chinese]
- 394 9. China Meteorology Administration (CMA, 2012). Notice of the China  
395 Meteorological Administration on the Issuance of Provisional Regulations on



- 396 Relocation and Removal of National ground meteorological observation Stations,  
397 *State Council Bulletin*, Retrieved from:  
398 [http://www.gov.cn/gongbao/content/2013/content\\_2344560.htm](http://www.gov.cn/gongbao/content/2013/content_2344560.htm). [In Chinese]
- 399 10. Dunn, R. J. H., Azorin-Molina, C., Menne, M. J., Zeng, Z., Casey, N. W., & Shen,  
400 C. (2022). Reduction in reversal of global stilling arising from correction to  
401 encoding of calm periods. *Environmental Research Communications*, **4**(6), 061003.
- 402 11. Feng, S., Hu, Q., & Qian, W. (2004). Quality control of daily meteorological data  
403 in China, 1951–2000: a new dataset. *International Journal of Climatology: A*  
404 *Journal of the Royal Meteorological Society*, **24**(7), 853-870.
- 405 12. Fu, G., Yu, J., Zhang, Y., Hu, S., Ouyang, R., & Liu, W. (2011). Temporal variation  
406 of wind speed in China for 1961–2007. *Theoretical and Applied Climatology*, **104**,  
407 313–324.
- 408 13. He, Y. C., Chan, P. W., & Li, Q. S. (2014). Standardization of raw wind speed  
409 data under complex terrain conditions: a data-driven scheme. *Journal of Wind*  
410 *Engineering and Industrial Aerodynamics*, **131**, 12-30.
- 411 14. Hong, H. P., Mara, T. G., Morris, R., Li, S. H., & Ye, W. (2014). Basis for  
412 recommending an update of wind velocity pressures in Canadian design codes.  
413 *Canadian Journal of Civil Engineering*, **41**(3), 206-221.
- 414 15. Hu, W., Kong, L., Zhu, X., & Xue, W. (2009). Accuracy analysis on contact  
415 anemometer self – recording records digitization processing system. *Journal of Arid*  
416 *Meteorology*, **27**, 168-171.
- 417 16. Jin, Rui. (2011). Difference of wind measurement data between automatic station  
418 and manual station. *Meteorological, Hydrological, and Oceanographic*  
419 *Instruments*, **3**, 16-18. [In Chinese]
- 420 17. Killick, R., Fearnhead, P., & Eckley, I. A. (2012). Optimal detection of  
421 changepoints with a linear computational cost. *Journal of the American Statistical*  
422 *Association*, **107**(500), 1590-1598.
- 423 18. Kuang, Yan. (2016). Application of magnetic rotary encoder in wind direction  
424 anemometer. *Civil Aviation Management*, **311**(9), 52-53. [In Chinese]



- 425 19. Li, Y., Chen, Y., Li, Z., & Fang, G. (2018). Recent recovery of surface wind speed  
426 in northwest China. *International Journal of Climatology*, **38**(12), 4445-4458.
- 427 20. Liu, F., Sun, F., Liu, W., Wang, T., Wang, H., Wang, X., & Lim, W. H. (2019). On  
428 wind speed pattern and energy potential in China. *Applied Energy*, **236**, 867–876.
- 429 21. Liu, X. (2000). The homogeneity test on mean annual wind speed over China.  
430 *Journal of Applied Meteorological Science*, **11**(1), 27-34.
- 431 22. Liu, Y. et al. (2022a). Increases in China's wind energy production from the  
432 recovery of wind speed since 2012, *Environmental Research Letters*, **17**(11).
- 433 23. Liu, Y., Xu, R., Ziegler, A. D. & Zeng, Z. (2022b). Stronger winds increase the  
434 sand-dust storm risk in northern China, *Environmental Science: Atmospheres*,  
435 online.
- 436 24. Masters, F. J., Vickery, P. J., Bacon, P., & Rappaport, E. N. (2010). Toward  
437 objective, standardized intensity estimates from surface wind speed observations.  
438 *Bulletin of the American Meteorological Society*, **91**(12), 1665-1682.
- 439 25. McVicar, T. R., Roderick, M. L., Donohue, R. J., Li, L. T., Van Niel, T. G., Thomas,  
440 A., ... & Dinpashoh, Y. (2012). Global review and synthesis of trends in observed  
441 terrestrial near-surface wind speeds: Implications for evaporation. *Journal of*  
442 *Hydrology*, **416**, 182-205.
- 443 26. Patzert, W., LaDochy, S., Ramirez, P., & Willis, J. (2016). Los Angeles Weather  
444 Station's relocation impacts climate and weather records.
- 445 27. Rayner, D. P. (2007). Wind run changes: the dominant factor affecting pan  
446 evaporation trends in Australia. *Journal of Climate*, **20**(14), 3379-3394.
- 447 28. Shen, C., Zha, J., Wu, J., & Zhao, D. (2021). Centennial-Scale Variability of  
448 Terrestrial Near-Surface Wind Speed over China from Reanalysis. *Journal of*  
449 *Climate*, **34**(14), 5829–5846. <https://doi.org/10.1175/JCLI-D-20-0436.1>
- 450 29. Sohu (2004 9.21). Due to lack of sufficient attention, 60% of the national ground  
451 meteorological observation stations were forced to relocate, *Domestic news*,  
452 Retrieved from: <https://news.sohu.com/20040921/n222160625.shtml>. [In Chinese]
- 453 30. Tamura, Y. (2009). Wind-induced damage to buildings and disaster risk reduction.



- 454 *Proceedings of the APCWE-VII, Taipei, Taiwan.*
- 455 31. Thiessen, A. H. (1911). Precipitation averages for large areas. *Monthly weather*  
456 *review*, **39**(7), 1082-1089.
- 457 32. Tian, Q., Huang, G., Hu, K., & Niyogi, D. (2019). Observed and global climate  
458 model based changes in wind power potential over the Northern Hemisphere  
459 during 1979–2016. *Energy*, **167**, 1224-1235.
- 460 33. Trewin, B. (2010). Exposure, instrumentation, and observing practice effects on  
461 land temperature measurements. *Wiley Interdisciplinary Reviews: Climate Change*,  
462 **1**(4), 490-506.
- 463 34. Vautard, R., Cattiaux, J., Yiou, P., Thépaut, J. N., & Ciais, P. (2010). Northern  
464 Hemisphere atmospheric stilling partly attributed to an increase in surface  
465 roughness. *Nature Geoscience*, **3**(11), 756-761.
- 466 35. Wan, H., Wang, X. L., & Swail, V. R. (2010). Homogenization and trend analysis  
467 of Canadian near-surface wind speeds. *Journal of Climate*, **23**(5), 1209-1225.
- 468 36. Wang, X. L. (2008). Accounting for autocorrelation in detecting mean shifts in  
469 climate data series using the penalized maximal t or F test. *Journal of Applied*  
470 *Meteorology and Climatology*, **47**(9), 2423-2444.
- 471 37. Wang, X., Piao, S., Ciais, P., Li, J., Friedlingstein, P., Koven, C., & Chen, A. (2011).  
472 Spring temperature change and its implication in the change of vegetation growth  
473 in North America from 1982 to 2006. *Proceedings of the National Academy of*  
474 *Sciences*, **108**(4), 1240-1245.
- 475 38. World Meteorological Organization (WMO, 2017). WMO guidelines on the  
476 calculation of climate normals. *WMO Technical Report*.  
477 [https://www.ncei.noaa.gov/pub/data/normals/WMO/Guidelines%20for%20the%20](https://www.ncei.noaa.gov/pub/data/normals/WMO/Guidelines%20for%20the%20Calculation%20of%20Climate%20Normals.WMO%20No1203_en.pdf)  
478 [0Calculation%20of%20Climate%20Normals.WMO%20No1203\\_en.pdf](https://www.ncei.noaa.gov/pub/data/normals/WMO/Guidelines%20for%20the%20Calculation%20of%20Climate%20Normals.WMO%20No1203_en.pdf)
- 479 39. World Meteorological Organization (WMO, 2020). Guidelines on homogenization.  
480 *WMO Technical Report*. [https://library.wmo.int/doc\\_num.php?explnum\\_id=10352](https://library.wmo.int/doc_num.php?explnum_id=10352)
- 481 40. Xin, Y., Chen, H., & Li, Y. (2012). Homogeneity adjustment of annual mean  
482 wind speed and elementary calculation of fundamental wind pressure over



- 483 Xinjiang meteorological stations. *Climatic and Environmental Research*, **17**(2),  
484 184-196. [In Chinese]
- 485 41. Yang, Jihua. (1986). The repair and maintenance of EL anemometer.  
486 *Meteorology of Xinjiang*, **8**, 46-47. [In Chinese]
- 487 42. Yang, M., Zhang, L., Cui, Y., Yang, Q., & Huang, B. (2019). The impact of wind  
488 field spatial heterogeneity and variability on short-term wind power forecast errors.  
489 *Journal of Renewable and Sustainable Energy*, **11**(3), 033304.
- 490 43. Yang, Q., Li, M., Zu, Z., & Ma, Z. (2021). Has the stilling of the surface wind speed  
491 ended in China? *Science China Earth Sciences*, **64**(7), 1036-1049.
- 492 44. Zeng, Z., Ziegler, A. D., Searchinger, T., Yang, L., Chen, A., Ju, K., ... & Wood, E.  
493 F. (2019). A reversal in global terrestrial stilling and its implications for wind  
494 energy production. *Nature Climate Change*, **9**(12), 979-985.
- 495 45. Zha, J., Shen, C., Zhao, D., Wu, J., & Fan, W. (2021). Slowdown and reversal of  
496 terrestrial near-surface wind speed and its future changes over eastern China.  
497 *Environmental Research Letters*, **16**(3), 034028. [https://doi.org/10.1088/1748-](https://doi.org/10.1088/1748-9326/abe2cd)  
498 [9326/abe2cd](https://doi.org/10.1088/1748-9326/abe2cd)
- 499 46. Zhang, G. et al. (2022). Rapid urbanization induced daily maximum wind speed  
500 decline in metropolitan areas: a case study in the Yangtze River Delta (China).  
501 *Urban Climate*, **43**, 101147.
- 502 47. Zhang, G., Azorin-Molina, C., Chen, D., Guijarro, J. A., Kong, F., Minola, L.,  
503 McVicar, T. R., Son, S., & Shi, P. (2020). Variability of Daily Maximum Wind  
504 Speed across China, 1975–2016: An Examination of Likely Causes, *Journal of*  
505 *Climate*, **33**(7), 2793-2816.
- 506 48. Zhou, Z., W, X., & Niu, R. (2002). Climate characteristics of sandstorm in China  
507 in recent 47 years. *Journal of Applied Meteorological Science*, **13**(2): 193-200.  
508